HHS Public Access

Author manuscript

Nat Neurosci. Author manuscript; available in PMC 2011 June 01.

Published in final edited form as:

Nat Neurosci. 2010 December ; 13(12): 1489–1495. doi:10.1038/nn.2667.

GRLD-1 regulates cell-wide abundance of glutamate receptor through post-transcriptional regulation

George J. Wang[1], **Lijun Kang**[2], **Julie E. Kim**[1], **Géraldine S. Maro**[1], **X. Z. Shawn Xu**[2], and **Kang Shen**[1]

[1]Department of Biology, Howard Hughes Medical Institute, Stanford University, 385 Serra Mall, California 94305, USA.

[2]Life Sciences Institute and Department of Molecular and Integrative Physiology, University of Michigan, 210 Washtenaw Avenue, Ann Arbor, MI 48109, USA.

Abstract

AMPA receptors mediate most of the fast postsynaptic response at glutamatergic synapses. The abundance of AMPA receptors in neurons and at postsynaptic membranes is tightly regulated. Changes in synaptic AMPA receptor levels have been proposed to be a key regulatory event in synaptic plasticity and learning and memory. While the local, synapse-specific regulation of AMPA receptors has been intensely studied, the global, cell-wide control is less well understood. Using a forward genetic approach, we identified Glutamate Receptor Level Decreased-1 (GRLD-1), a putative RNA-binding protein that is required for efficient production of GLR-1 in the AVE interneurons in the nematode *Caenorhabditis elegans*. In *grld-1* mutants, GLR-1 levels were drastically reduced. Consistently, both glutamate-induced currents in AVE and *glr-1*-dependent nose-touch avoidance behavior were defective in *grld-1* mutants. We propose that this evolutionarily conserved family of proteins controls the abundance of GLR-1 by regulating *glr-1* transcript splicing.

The α-amino-3-hydroxy-5-methyl-4-isoxazolepropionic acid (AMPA)-type glutamate receptors are ligand-gated ion channels that mediate the majority of fast excitatory neurotransmission in the brain. Therefore, the abundance of surface AMPA receptors at the synapse and their conductance are key determinants of synaptic strength for glutamatergic synapses. It is widely accepted that regulation of AMPA receptors at individual synapses is one of the core molecular mechanisms underlying synaptic plasticity and learning and memory[1].

In addition to synapse-specific plasticity, another form of plasticity occurs at the whole-neuron level. Neurons must coordinate synaptic strength at the whole-cell level over time in

Correspondence and requests for materials should be addressed to K.S. (kangshen@stanford.edu).

Author Contributions

G.J.W. performed most of the experiments. X.Z.S.X. supervised L.K. who did the electrophysiological experiments. J.E.K. contributed to the initial screen and transgene development. G.S.M. contributed to the intron experiments. K.S., G.J.W., and G.S.M. analyzed the data and wrote the manuscript.

order to prevent destabilizing feedback loops. The input-specific potentiation of synaptic strength must be scaled by cell-wide homeostatic mechanisms. The regulation of AMPA receptor abundance has also been implicated as an important molecular mechanism for this type of synaptic scaling[2,3].

We chose to study AMPA receptor regulation by focusing on the AMPA receptor GLR-1 in *C. elegans*, the closest homolog to vertebrate AMPA receptor subunits. GLR-1 is found in ~10% of the 302 neurons in the worm[4–6] and is necessary for many behaviors including hyperosmotic avoidance, tactile avoidance, foraging, and long-term memory[7]. Previous studies suggest that homeostatic synaptic scaling also occurs with GLR-1 in *C. elegans*, because loss of evoked synaptic neurotransmitter release in mutants of *unc-2*, a voltage-dependent calcium channel, and *eat-4*, a vesicular glutamate transporter, both lead to increased GLR-1 levels[8]. In addition, a number of studies have focused on the abundance of GLR-1 in many neurons in the *C. elegans* ventral nerve cord identifying regulators such as LIN-10[9], CaMKII[10], and the ubiquitin proteasome system[11,12].

In order to discover new regulators of GLR-1 abundance, we studied GLR-1 in two bilaterally symmetric command interneurons, AVEL and AVER (subsequently referred to as AVE). While previous studies have looked at GLR-1 in many neurons within the ventral cord, we hypothesized that studying GLR-1 with single-cell resolution would yield new regulators. Using a forward genetics approach, we found a new post-transcriptional regulator of GLR-1, GRLD-1, a member of the conserved RNA-binding family of SPEN proteins, which positively regulates GLR-1 levels. Rescue experiments expressing cDNA and genomic constructs suggest that GRLD-1 may function through splicing of the *glr-1* transcript.

Results

grld-1 mutants exhibit reduced GLR-1 levels in AVE

To explore the molecular mechanisms that regulate the level of glutamate receptors *in vivo*, we utilized a previously described functional, fluorescently-tagged GLR-1 protein[9,10,13]. We visualized GLR-1 *in vivo* in the bilaterally symmetrical backward command interneurons AVE by expressing GLR-1::YFP driven by the *opt-3* promoter[14] (Fig. 1a). Serial electron microscopic (EM) reconstruction shows that the proximal segment of AVE in the nerve ring is exclusively postsynaptic while the distal portion of the process in the ventral cord is predominantly presynaptic[15]. AVE receives synaptic input from sensory neurons and interneurons. Together with the other two backward command neurons AVA and AVD, AVE innervates A-type motor neurons[16] (Fig. 1b). When animals collide nose-on with an object, they respond by initiating backward movement, which is mediated by these backward command neurons. *glr-1* is expressed in AVE, and the nose-touch behavior is defective in *glr-1* mutants, suggesting that glutamatergic transmission is required for the behavioral function of AVE[4–6].

Consistent with the EM data, GLR-1::YFP fluorescence localized predominantly in the proximal segment of the AVE process, while presynaptic markers, such as SNB-1, localized to the distal axonal segment (Fig. 1c, Supplementary Fig. 1d). To identify novel regulators

of GLR-1 expression, we performed a visual forward genetic screen for mutants in which GLR-1::YFP levels were affected in AVE. From the screen, we isolated two recessive mutants, *wy225* and *wy655*, which exhibited a drastic reduction of GLR-1::YFP levels in the AVE "dendrite" in both developing and mature animals. Non-complementation experiments showed that the two alleles were in the same complementation group, which we named *grld-1*. When compared with wild-type controls, *grld-1(wy225)* and *grld-1(wy655)* animals had a 68.3% (n = 54) and 72.7% (n = 22) reduction, respectively, in GLR-1::YFP level in the AVE proximal segment in L2-stage worms (Fig. 1c–e). In the cell bodies of AVE, we found a 79.5% reduction of GLR-1::YFP in L2-stage worms (*grld-1(wy225)*, n = 23). The reduction in GLR-1::YFP persisted during the lifespan of the animal with a 51% reduction in L4-stage and young adults (Fig. 7b). The polarized distribution of GLR-1 to the dendritic segment was not affected, because ectopic GLR-1::YFP fluorescence was not observed in the axon (data not shown).

In order to understand how *grld-1* mutations affect AVE, we first examined the general morphology of the neuron. Expression of cytoplasmic mCherry driven by the *opt-3* promoter showed that the AVE cell body was normally localized and that the outgrowth and guidance of the AVE neurite was not affected (Supplementary Fig. 1a, b). In addition, the expression level of mCherry was not decreased in *grld-1(wy225)* animals indicating that the *opt-3* promoter is not affected by the *grld-1* mutation and is not likely to be the cause of the reduced GLR-1::YFP (Supplementary Fig. 1c, n = 35).

Next we examined whether the general axon-dendrite polarity of AVE was still intact. We found that the expression level and localization of a synaptic vesicle protein SNB-1::CFP in AVE was not affected in *grld-1(wy225)* mutants (Supplementary Fig. 1d, e). The localization and expression of another somato-dendritically localized protein, ROR receptor tyrosine kinase CAM-1::YFP[17,18], was also not affected in *grld-1(wy225)* mutants (Supplementary Fig. 1f–h). Taken together, these experiments suggest that GRLD-1 specifically regulates the expression level of GLR-1.

Next we asked if the expression of fluorescently-tagged GLR-1 in other neurons was also affected in *grld-1* mutants. GLR-1::GFP expressed under the *glr-1* promoter was not grossly affected (data not shown). Because the *glr-1* promoter is expressed in many neurons, it was difficult to determine whether GLR-1 levels were reduced in a subset of neurons including AVE. We, therefore, examined expression of GLR-1::GFP in another interneuron, RIA, and found no effect in *grld-1(wy225)* mutants (data not shown). Thus, *grld-1* appears to be required for expression of GLR-1 specifically in AVE.

Since AVE is a backward command interneuron involved in the nose-touch avoidance behavior, we reasoned that the reduction in GLR-1 level might affect this behavior. Consistent with previous reports[4,9], wild-type worms displayed an avoidance response of 66.8%, while *glr-1(n2461)* worms had an avoidance response of 16.4% (Fig. 2a). Interestingly, *grld-1(wy225)* mutants had an avoidance response of 9.7%, significantly less than both wild-type and *glr-1(n2461)*, suggesting that *grld-1* is required for the nose-touch avoidance behavior (Fig. 2a).

While the reduction of GLR-1::YFP in the *grld-1* mutant indicates an overall decrease in the amount of GLR-1, the fluorescence readout does not distinguish between functional surface receptors and receptors in the internal stores. To directly measure functional GLR-1 in AVE, we used *in vivo* whole-cell patch-clamp techniques to record glutamate-gated currents in AVE. Exogenously applied glutamate from a pressured pipette typically induced an inward current in AVE, with average amplitude of 34 pA/pF in wild-type animals (Fig. 2b, d). In *grld-1* mutants, the amplitude of the glutamate-induced inward currents was significantly reduced (6.8 pA/pF, Fig. 2c, d). The overall voltage-dependent membrane currents in AVE were similar in wild-type and *grld-1(wy225)* animals, suggesting that the general electrophysiological properties and healthiness of AVE were not changed (Supplementary Fig. 2). Taken together, these results argue that GRLD-1 plays an essential role in generating appropriate amounts of functional glutamate receptors on the cell surface.

GRLD-1 is a SPEN family RNA-binding protein

We identified the mutations responsible for both the *grld-1(wy225)* and *grld-1(wy655)* phenotypes in the predicted gene F29C4.7 by genetic mapping and transformation rescue (data not shown). The molecular lesion for *grld-1(wy225)* is a G to A transition that disrupts the splice donor site for intron 4 (Fig. 3a). Without proper splicing of intron 4, GRLD-1 is predicted to be truncated with the addition of three amino acids followed by an in-frame stop codon in the unspliced intron 4. The molecular lesion for *grld-1(wy655)* is a G to T transversion that results in a stop codon - G397Stop (Fig. 3a). In addition, we also performed RNA interference (RNAi) of F29C4.7 and found GLR-1::YFP levels in AVE reduced by 57.0% (Supplementary Fig. 3). These results argue that both *grld-1* alleles represent loss-of-function alleles.

grld-1 encodes a putative RNA-binding protein of the conserved *split ends (Spen)* family (Fig. 3b). SPEN proteins are characterized by three N-terminal RNA recognition motifs (RRMs) and a C-terminal SPOC (SPEN paralog and ortholog C-terminal domain) domain (Fig. 3a)[19]. Worms, flies, mice, and humans all have at least two types of SPEN family members: a short-form (to which GRLD-1 belongs) and a long-form (Fig. 3a). In *C. elegans*, *grld-1* is the sole short-form member and has not been previously studied. *din-1L* is the only long-form member in *C. elegans*.[20] We found that *din-1L(hd36)* does not reduce the levels of GLR-1::YFP in AVE (data not shown) and RNAi of *din-1L* also did not reduce the levels of GLR-1::YFP in AVE (Supplementary Fig. 3).

GRLD-1 is expressed widely and localizes to the nucleus

Next we determined the expression pattern of *grld-1* by utilizing fosmid recombineering[21] to engineer an in-frame GFP at the C-terminus of the *grld-1* open-reading frame. We found that *grld-1* was expressed in many cell types including, muscles, epithelial cells, and neurons. By co-expressing mCherry under the *opt-3* promoter, we found that *grld-1* was expressed in AVE (Fig. 3c). *grld-1* was also expressed in many of the neurons important for the nose-touch behavior including the A-type motor neurons, the sensory neuron, ASH, and the *glr-1*-expressing interneurons AVA and AVD (Supplementary Fig. 4a–c).

We next examined GRLD-1 subcellular localization in AVE by expressing GRLD-1 N-terminally-tagged with GFP under the *opt-3* promoter. GFP::GRLD-1 exclusively localized to the nucleus of AVE (Fig. 3d–f). This is similar to the localization of GRLD-1 homologs[19,22–25] and is consistent with a role for GRLD-1 in regulating RNA.

GRLD-1 functions cell-autonomously in AVE

In order to determine in what cells *grld-1* functions to regulate GLR-1 levels in AVE, we expressed *grld-1* cDNA using the *opt-3* promoter in *grld-1* mutants. We found that transgenic animals not only rescued the fluorescence defect but also expressed GLR-1 at a significantly higher level compared to wild-type animals (Fig. 4a). Similarly, expression of *grld-1* in *grld-1(wy225)* mutants under the *nmr-1* promoter, which is expressed in AVE but in no other cells that overlap with the *opt-3* promoter, showed rescue of GLR-1 levels in AVE (data not shown). These data suggest that GRLD-1 functions cell-autonomously in AVE to regulate the level of GLR-1.

Furthermore, cell-autonomous expression of *grld-1* also significantly rescued the nose-touch defects in *grld-1* mutants (Fig. 4b). Mutant animals expressing *Popt-3::grld-1* at a higher level (50 ng/ul) exhibited a higher level of behavioral rescue compared with animals expressing a lower level (20 ng/ul) of the same transgene (Fig. 4b), implying that high dose of GRLD-1 can lead to high levels of GLR-1.

The rescue of the behavioral defect was not complete, even in strains where the fluorescent GLR-1 level in AVE were higher than in our initial GLR-1::YFP-expressing line. We considered two possible explanations for the discrepancy between the higher than normal GLR-1::GFP in AVE and the incomplete behavioral rescue. One was that the high GLR-1::GFP might not represent functional receptor on the cell surface. To directly test this idea, we recorded glutamate-induced excitatory current from AVE in *grld-1(wy225)* mutants expressing *Popt-3::grld-1* (50 ng/ul). We found that expression of *grld-1* in AVE was able to rescue the glutamate-gated current in AVE to wild-type levels (Fig. 4c, d). The inward current was not significantly higher than wild-type levels suggesting that there are additional mechanisms that control the membrane insertion of GLR-1 in AVE. Nevertheless, the rescue in current demonstrates that the function of AVE is likely rescued in these cell-autonomously rescued animals.

The second possibility we considered was that additional *grld-1* expressing cells (other than AVE) are required for the nose-touch avoidance behavior. Because our expression analysis showed that *grld-1* was expressed in other *glr-1*-expressing neurons, we tested whether expression of *grld-1* in *glr-1*-expressing neurons could rescue the behavior. We found that these strains also partially rescued the nose-touch behavior but not to wild-type levels (Supplementary Fig. 5). A number of reasons may explain the lack of complete rescue including the requirement of *grld-1* in *glr-1* negative cells in the nose-touch circuit, and the improper temporal regulation or magnitude of expression due to the *glr-1* promoter.

The RRM domains are sufficient to rescue GLR-1 levels

To understand which domains of GRLD-1 are necessary for GRLD-1 function, we created two truncated cDNA constructs expressed under the *opt-3* promoter in *grld-1* mutants: one with the RRM domains (amino acids 1–375) and one with the SPOC domain (amino acids 322–520). Expression of the RRMs completely rescued the GLR-1 defect in *grld-1* mutants (Fig. 5). Expression of the SPOC domain increased the levels of GLR-1 in *grld-1* mutants, but the levels were still significantly below that of wild-type controls (Fig. 5).

There is an apparent discrepancy between the ability for the RRMs to rescue the GLR-1 defect and our *grld-1* mutations that both result in stop codons after the RRMs. One reason for this discrepancy could be the degradation of *grld-1* transcripts in the *grld-1* mutants caused by nonsense-mediated decay (NMD). Therefore, we blocked NMD with the null *smg-3(r930)* mutation[26] in *grld-1(wy225)* mutants. The levels of GLR-1 in the *smg-3(r930)*; *grld-1(wy225)* double mutants were similar to *grld-1(wy225)* mutants (data not shown), suggesting that the *grld-1* transcript is not degraded by NMD. We speculate another possible reason for the RRMs alone to rescue is that the *wy225* and *wy655* mutations result in truncated GRLD-1 with reduced activity not sufficient for wild-type expression of GLR-1, whereas overexpressed levels of GRLD-1 RRMs are sufficient for high expression of GLR-1.

GRLD-1 functions through the *glr-1* introns

Since the RRM domains, which are known to bind RNAs, were sufficient to rescue the phenotype of *grld-1* mutants, we hypothesized that GRLD-1 functions by regulating the *glr-1* RNA. This hypothesis is consistent with previous work showing that AMPA receptor RNA is regulated[1]. Because many transcripts have been shown to be regulated and stabilized through their 3' UTRs[27,28], we first wanted to determine whether the *glr-1 3' UTR* was necessary for GRLD-1 to regulate GLR-1 levels. We reasoned that if the *glr-1 3' UTR* was indeed required for proper GLR-1 levels through GRLD-1, then *glr-1* with a different 3' UTR would bypass the need for GRLD-1. We decided to use the *unc-10/RIM 3' UTR*, because we had already shown that *cam-1::unc-10 3' UTR* expression was not reduced in *grld-1* mutants (Supplementary Fig. 1f–h).

The *glr-1* transgene used in the experiments described thus far was the genomic fragment of *glr-1* that included all the introns as well as the endogenous 3' UTR (Fig. 6a). We replaced the 3' UTR with the *unc-10 3' UTR*, thus making [*glr-1 genomic::yfp::unc-10 3' UTR*] (Fig. 6b). In two independent transgenic lines expressing *glr-1* with the *unc-10 3' UTR*, the fluorescence intensity was lower in the *grld-1* mutants compared to the wild-type background to a similar degree as seen with the construct carrying the *glr-1* endogenous 3' UTR (Fig. 6d, e, h). This result indicates that GLR-1 can still be regulated by GRLD-1 independent of the 3' UTR and that the 3' UTR of *glr-1* is not required for its regulation by GRLD-1.

We next hypothesized that GRLD-1 may regulate the *glr-1* transcript through the *glr-1* introns. For example, GRLD-1 may be required to splice out an intron and without this splicing GLR-1 levels are lowered. We thus made [*glr-1 cDNA::gfp::glr-1 3' UTR*], which

contained the *glr-1* cDNA without any introns followed by the *glr-1 3' UTR* (Fig. 6c). Interestingly, the GLR-1 fluorescence resulting from the cDNA constructs was similar in *grld-1* mutants compared to wild-type animals (Fig. 6f–h). In other words, the requirement for GRLD-1 regulation was largely absent for the [*glr-1 cDNA::gfp::glr-1 3' UTR*] expressing strains. Since the only difference between the genomic construct and the cDNA construct was the presence of introns, this result suggests that GRLD-1 may be required for proper generation of mature mRNA in AVE.

If wild-type levels of GLR-1 protein can be achieved by expression of *glr-1* cDNA even in the absence of *grld-1*, then we hypothesized that *glr-1* cDNA should be able to rescue the nose-touch behavior in *grld-1* mutants. Additionally, the *glr-1* genomic construct with introns should not rescue the behavioral defect. To test these predictions, we used the nose-touch behavioral assay to test *grld-1* mutants expressing either the cDNA construct or the genomic construct. We indeed observed significant rescue in *grld-1* mutants that expressed the cDNA but not the genomic construct (Fig. 6i). The ability for expression of *glr-1* in *grld-1(wy225)* to rescue the nose-touch behavior also suggests that specific loss of *glr-1* in AVE of *grld-1* mutants is an important cause of the nose-touch defect.

These results led us to hypothesize that GRLD-1 regulates the splicing of *glr-1*. We speculated that GRLD-1 may be required to splice a specific set of *glr-1*'s 13 introns or may be required to splice any intron in *glr-1*. To test these two possibilities, we constructed three genomic-cDNA hyrbids of *glr-1: [glr-1 genomic (minus introns 1–2)::gfp::glr-1 3' UTR]*, [*glr-1 genomic (minus introns 3–9)::gfp::glr-1 3' UTR*], and [*glr-1 genomic (minus introns 10–13)::gfp::glr-1 3' UTR*]. We found that without introns 1–2 the requirement of GRLD-1 for GLR-1 expression was largely reduced, however, constructs lacking introns 3–9 or 10–13 still required GRLD-1 for normal GLR-1 expression (Supplementary Fig. 6c–e, 6g). These findings suggest the splicing of *glr-1* introns 1–2 is critical for proper expression of GLR-1 and this splicing requires GRLD-1. To further test if introns 1–2 were sufficient to enlist the control by GRLD-1, we constructed a genomic-cDNA hybrid containing only introns 1–2 [*glr-1 genomic (minus introns 3–13)::gfp::glr-1 3' UTR*]. This construct, similar to the genomic construct produced low levels of GLR-1 in the absence of GRLD-1 (Supplementary Fig. 6f–g).

Taken together, these data argue that GRLD-1 is regulating the splicing of *glr-1*, specifically the removal of introns 1–2, and is required for the efficient generation of mature *glr-1* mRNA in AVE. A direct test of this hypothesis would be to compare the level of *glr-1* mRNA in the mutant and the wild-type animals. We used quantitative RT-PCR to measure the total *glr-1* mRNA in the entire animal and found no significant difference between wild-type and *grld-1* mutants (data not shown). However, *glr-1* is expressed in many neurons[4–6] and GRLD-1 might only regulate *glr-1* in a small subset of cells. Indeed, we examined GLR-1 levels in all *glr-1*- expressing neurons using the *glr-1* promoter and found that GLR-1 levels were not broadly decreased (data not shown). Hence, additional proteins might play similar functions in neurons other than AVE.

GRLD-1 maintains GLR-1 levels after AVE development

We next tested whether GRLD-1 was only necessary during the initial establishment of GLR-1 levels in AVE or whether GRLD-1 played a role in maintaining levels of GLR-1. We created transgenic lines expressing *grld-1* under the heat-shock inducible promoter (*Phs*) in *grld-1* mutants[29] and performed a two-hour heat-shock of L2-staged animals, in which the AVE axon and dendrite formation is already completed, and then scored the phenotype in the L4-young adult stage 18 hours later (Fig. 7a). Heat-shocked transgenic animals with *Phs::grld-1* completely rescued the GLR-1 phenotype in the *grld-1* mutants (Fig. 7b). Heat-shocked mutants without the transgene or non-heat-shocked animals with the heat-shock transgene were not significantly different from *grld-1* mutants (Fig. 7b). These data suggest that there is an ongoing requirement for GRLD-1 to maintain GLR-1 levels after development has been completed.

Discussion

The regulation of AMPA receptors plays a key role in learning and memory. Our study shows that GRLD-1 is a novel *C. elegans* SPEN protein that is required to maintain normal levels of the AMPA receptor, GLR-1, throughout the cell. GRLD-1 acts cell-autonomously to regulate GLR-1 levels and likely functions by splicing *glr-1* introns 1–2.

The SPEN family of proteins is comprised of long-form and short-form members. Humans, mice, flies, and worms all have at least one long-form and one short-form, while humans and mice have an additional short-form homolog. Both the mouse long-form and the short-forms are expressed in the brain[30]. However, relatively little is known about the functions of the SPEN protein family, especially in the context of neurobiology. A conditional mouse knockout allele of *mint* exhibits brain growth retardation and hypoplasia by 8 weeks of age, likely due to postnatal neuronal cell death[31]. In *Drosophila*, the long-form, SPEN, regulates neuronal cell fate and axon guidance through the Notch and EGFR pathways[19,32]. The *Drosophila* short-form, *nito*, plays a role in proper eye size development both antagonistically[33] and cooperatively[34] with SPEN.

We now provide evidence that a member of the SPEN family, GRLD-1 regulates the abundance of AMPA receptors. Multiple lines of evidence support this claim: reduction of GLR-1::YFP in *grld-1* mutants, lack of behavioral response in the nose-touch assay in *grld-1* mutants, diminished glutamate-gated currents in *grld-1(wy225)* mutants, and increased GLR-1 levels upon over-expression of GRLD-1. These data show that GRLD-1 is a positive regulator of GLR-1.

SPEN family proteins are characterized by three N-terminal RRM domains and a C-terminal SPOC domain. RRM domains are implicated in many aspects of RNA biology splicing, stability, editing, translational regulation, and degradation[35]. The long-form SPEN homologs are implicated in many studies as transcriptional regulators downstream of Notch/RBP-Jk, Wnt, EGFR, and nuclear receptor pathways[19,25,31,34,36,37]. However, there is less evidence for transcriptional regulation by the short-form members of the SPEN family and more evidence for RNA regulation. The mouse protein, OTT1, binds the RNA of the RNA transport element (RTE, found in mouse retrotransposons) and promotes nuclear export and

expression of RTE-containing reporter mRNAs[38]. OTT1 also binds the protein NXF1[38], and the viral protein EB2[23], which are both involved in nuclear export of mRNA. Additionally, OTT1 is found in the human spliceosome[39]. Similarly, human OTT3 may play a role in splicing because its ectopic expression in cultured cells represses alternative splicing of beta-thalassemia[23].

Our findings are consistent with previous studies indicating that short-form SPEN proteins function in post-transcriptional RNA regulation. To further elucidate the role of GRLD-1, we demonstrated that expression of intronless *glr-1* cDNA resulted in near wild-type GLR-1 levels in *grld-1* mutants. The *glr-1* cDNA construct could also rescue the *grld-1(wy225)* nose-touch behavioral defect, showing that GLR-1 levels were also functionally rescued. The removal of *glr-1* introns, specifically introns 1–2, bypassed the need for *grld-1* and resulted in increased levels of GLR-1 in *grld-1* mutants. In many aspects, introns and their splicing promote protein levels by harboring transcriptional enhancer elements and facilitating processes such as polyadenylation, mRNA nuclear export, and translation[40,41]. However, our results suggest that introns 1–2 in *glr-1* negatively regulate protein levels of GLR-1. Based on these results, we hypothesize that GRLD-1 is a specific splice factor for *glr-1* introns 1–2 in AVE. The nuclear localization of fluorescently-tagged GRLD-1 supports the hypothesis that GRLD-1 functions as a splicing factor. Future RNA-binding and splicing assays will be needed to directly test this model.

Our heatshock experiments showed that expressing *grld-1* late, after AVE development is complete, is sufficient to rescue GLR-1 levels. This suggests a maintenance role for GRLD-1 in calibrating levels of GLR-1, which is intriguing given the importance of AMPA receptors in memory and learning. These experience-dependent events rely on modulation of AMPA receptor abundance and occur after the initial development of neurons has taken place. Previous studies implicate RNA splicing of NMDA-type glutamate receptors in the regulation of receptor abundance for homeostatic synaptic scaling. Alternative splicing of the NMDA receptors results in different speeds of ER export and subsequent receptor levels at the synapse[42]. Thus it will be of great interest to determine if GRLD-1 plays an experience-dependent role in controlling the levels of AMPA receptors.

Supplementary Material

Refer to Web version on PubMed Central for supplementary material.

Acknowledgements

This work was supported by the Human Frontier Science Foundation, the W. M. Keck Foundation and the Howard Hughes Medical Institute (K.S.); the Pew Scholar Award and NIH (X.Z.S.X.); and the NSF-GRFP and the Burt and Deedee McMurtry Stanford Graduate Fellowship (G.J.W.). We thank the International *Caenorhabditis* Genetic Center for strains and the Antebi and Kaplan labs for strains and constructs. We also thank Q. Hu, C. Gao, F. Chen and Y. Fu for assistance and members of the Shen laboratory for comments on the manuscript.

References

1. Shepherd JD, Huganir RL. The cell biology of synaptic plasticity: AMPA receptor trafficking. Annu Rev Cell Dev Biol. 2007; 23:613–643. [PubMed: 17506699]

2. Turrigiano GG, Leslie KR, Desai NS, Rutherford LC, Nelson SB. Activity-dependent scaling of quantal amplitude in neocortical neurons. Nature. 1998; 391:892–896. [PubMed: 9495341]
3. Maghsoodi B, et al. Retinoic acid regulates RARalpha-mediated control of translation in dendritic RNA granules during homeostatic synaptic plasticity. Proc Natl Acad Sci U S A. 2008; 105:16015–16020. [PubMed: 18840692]
4. Hart AC, Sims S, Kaplan JM. Synaptic code for sensory modalities revealed by C. elegans GLR-1 glutamate receptor. Nature. 1995; 378:82–85. [PubMed: 7477294]
5. Brockie PJ, Madsen DM, Zheng Y, Mellem J, Maricq AV. Differential expression of glutamate receptor subunits in the nervous system of Caenorhabditis elegans and their regulation by the homeodomain protein UNC-42. J Neurosci. 2001; 21:1510–1522. [PubMed: 11222641]
6. Maricq AV, Peckol E, Driscoll M, Bargmann CI. Mechanosensory signalling in C. elegans mediated by the GLR-1 glutamate receptor. Nature. 1995; 378:78–81. [PubMed: 7477293]
7. Brockie PJ, Maricq AV. Ionotropic glutamate receptors: genetics, behavior and electrophysiology. WormBook. 2006:1–16. [PubMed: 18050468]
8. Grunwald ME, Mellem JE, Strutz N, Maricq AV, Kaplan JM. Clathrin-mediated endocytosis is required for compensatory regulation of GLR-1 glutamate receptors after activity blockade. Proc Natl Acad Sci U S A. 2004; 101:3190–3195. [PubMed: 14981253]
9. Rongo C, Whitfield CW, Rodal A, Kim SK, Kaplan JM. LIN-10 is a shared component of the polarized protein localization pathways in neurons and epithelia. Cell. 1998; 94:751–759. [PubMed: 9753322]
10. Rongo C, Kaplan JM. CaMKII regulates the density of central glutamatergic synapses in vivo. Nature. 1999; 402:195–199. [PubMed: 10647013]
11. Juo P, Kaplan JM. The anaphase-promoting complex regulates the abundance of GLR-1 glutamate receptors in the ventral nerve cord of C. elegans. Curr Biol. 2004; 14:2057–2062. [PubMed: 15556870]
12. Burbea M, Dreier L, Dittman JS, Grunwald ME, Kaplan JM. Ubiquitin and AP180 regulate the abundance of GLR-1 glutamate receptors at postsynaptic elements in C. elegans. Neuron. 2002; 35:107–120. [PubMed: 12123612]
13. Zheng Y, Mellem JE, Brockie PJ, Madsen DM, Maricq AV. SOL-1 is a CUB-domain protein required for GLR-1 glutamate receptor function in C. elegans. Nature. 2004; 427:451–457. [PubMed: 14749834]
14. Fei YJ, et al. A novel H(+)-coupled oligopeptide transporter (OPT3) from Caenorhabditis elegans with a predominant function as a H(+) channel and an exclusive expression in neurons. J Biol Chem. 2000; 275:9563–9571. [PubMed: 10734106]
15. White JG, Southgate E, Thomson JN, Brenner S. The structure of the nervous system *Caenorhabditis elegans*. Philosophical Transactions of the Royal Society of London. 1986; 314:1–340. [PubMed: 22462104]
16. Riddle, DL. C. elegans II. Plainview, N.Y.: Cold Spring Harbor Laboratory Press; 1997.
17. Paganoni S, Ferreira A. Expression and subcellular localization of Ror tyrosine kinase receptors are developmentally regulated in cultured hippocampal neurons. J Neurosci Res. 2003; 73:429–440. [PubMed: 12898527]
18. Sieburth D, et al. Systematic analysis of genes required for synapse structure and function. Nature. 2005; 436:510–517. [PubMed: 16049479]
19. Kuang B, Wu SC, Shin Y, Luo L, Kolodziej P. split ends encodes large nuclear proteins that regulate neuronal cell fate and axon extension in the Drosophila embryo. Development. 2000; 127:1517–1529. [PubMed: 10704397]
20. Ludewig AH, et al. A novel nuclear receptor/coregulator complex controls C. elegans lipid metabolism, larval development, and aging. Genes Dev. 2004; 18:2120–2133. [PubMed: 15314028]
21. Tursun B, Cochella L, Carrera I, Hobert O. A toolkit and robust pipeline for the generation of fosmid-based reporter genes in C. elegans. PLoS One. 2009; 4:e4625. [PubMed: 19259264]
22. Ma X, et al. Rbm15 modulates Notch-induced transcriptional activation and affects myeloid differentiation. Mol Cell Biol. 2007; 27:3056–3064. [PubMed: 17283045]

23. Hiriart E, et al. Interaction of the Epstein-Barr virus mRNA export factor EB2 with human Spen proteins SHARP, OTT1, and a novel member of the family, OTT3, links Spen proteins with splicing regulation and mRNA export. J Biol Chem. 2005; 280:36935–36945. [PubMed: 16129689]
24. Oswald F, et al. SHARP is a novel component of the Notch/RBP-Jkappa signaling pathway. EMBO J. 2002; 21:5417–5426. [PubMed: 12374742]
25. Shi Y, et al. Sharp, an inducible cofactor that integrates nuclear receptor repression and activation. Genes Dev. 2001; 15:1140–1151. [PubMed: 11331609]
26. Johns L, Grimson A, Kuchma SL, Newman CL, Anderson P. Caenorhabditis elegans SMG-2 selectively marks mRNAs containing premature translation termination codons. Mol Cell Biol. 2007; 27:5630–5638. [PubMed: 17562857]
27. Bolognani F, Perrone-Bizzozero NI. RNA-protein interactions and control of mRNA stability in neurons. J Neurosci Res. 2008; 86:481–489. [PubMed: 17853436]
28. Merritt C, Rasoloson D, Ko D, Seydoux G. 3' UTRs are the primary regulators of gene expression in the C. elegans germline. Curr Biol. 2008; 18:1476–1482. [PubMed: 18818082]
29. Stringham EG, Dixon DK, Jones D, Candido EP. Temporal and spatial expression patterns of the small heat shock (hsp16) genes in transgenic Caenorhabditis elegans. Mol Biol Cell. 1992; 3:221–233. [PubMed: 1550963]
30. Lein ES, et al. Genome-wide atlas of gene expression in the adult mouse brain. Nature. 2007; 445:168–176. [PubMed: 17151600]
31. Yabe D, et al. Generation of a conditional knockout allele for mammalian Spen protein Mint/SHARP. Genesis. 2007; 45:300–306. [PubMed: 17457934]
32. Kolodziej PA, Jan LY, Jan YN. Mutations that affect the length, fasciculation, or ventral orientation of specific sensory axons in the Drosophila embryo. Neuron. 1995; 15:273–286. [PubMed: 7646885]
33. Jemc J, Rebay I. Characterization of the split ends-like gene spenito reveals functional antagonism between SPOC family members during Drosophila eye development. Genetics. 2006; 173:279–286. [PubMed: 16547102]
34. Chang JL, Lin HV, Blauwkamp TA, Cadigan KM. Spenito and Split ends act redundantly to promote Wingless signaling. Dev Biol. 2008; 314:100–111. [PubMed: 18174108]
35. Maris C, Dominguez C, Allain FH. The RNA recognition motif, a plastic RNA-binding platform to regulate post-transcriptional gene expression. FEBS J. 2005; 272:2118–2131. [PubMed: 15853797]
36. Feng Y, et al. Drosophila split ends homologue SHARP functions as a positive regulator of Wnt/beta-catenin/T-cell factor signaling in neoplastic transformation. Cancer Res. 2007; 67:482–491. [PubMed: 17234755]
37. Kuroda K, et al. Regulation of marginal zone B cell development by MINT, a suppressor of Notch/RBP-J signaling pathway. Immunity. 2003; 18:301–312. [PubMed: 12594956]
38. Lindtner S, et al. RNA-binding motif protein 15 binds to the RNA transport element RTE and provides a direct link to the NXF1 export pathway. J Biol Chem. 2006; 281:36915–36928. [PubMed: 17001072]
39. Zhou Z, Licklider LJ, Gygi SP, Reed R. Comprehensive proteomic analysis of the human spliceosome. Nature. 2002; 419:182–185. [PubMed: 12226669]
40. Moore MJ, Proudfoot NJ. Pre-mRNA processing reaches back to transcription and ahead to translation. Cell. 2009; 136:688–700. [PubMed: 19239889]
41. Le Hir H, Nott A, Moore MJ. How introns influence and enhance eukaryotic gene expression. Trends Biochem Sci. 2003; 28:215–220. [PubMed: 12713906]
42. Mu Y, Otsuka T, Horton AC, Scott DB, Ehlers MD. Activity-dependent mRNA splicing controls ER export and synaptic delivery of NMDA receptors. Neuron. 2003; 40:581–594. [PubMed: 14642281]
43. Goodman MB, Hall DH, Avery L, Lockery SR. Active currents regulate sensitivity and dynamic range in C. elegans neurons. Neuron. 1998; 20:763–772. [PubMed: 9581767]
44. Mello C, Fire A. DNA transformation. Methods Cell Biol. 1995; 48:451–482. [PubMed: 8531738]

45. Girard LR, et al. WormBook: the online review of Caenorhabditis elegans biology. Nucleic Acids Res. 2007; 35:D472–D475. [PubMed: 17099225]
46. Wang D, et al. Somatic misexpression of germline P granules and enhanced RNA interference in retinoblastoma pathway mutants. Nature. 2005; 436:593–597. [PubMed: 16049496]
47. Poon VY, Klassen MP, Shen K. UNC-6/netrin and its receptor UNC-5 locally exclude presynaptic components from dendrites. Nature. 2008; 455:669–673. [PubMed: 18776887]
48. Brockie PJ, Mellem JE, Hills T, Madsen DM, Maricq AV. The C. elegans glutamate receptor subunit NMR-1 is required for slow NMDA-activated currents that regulate reversal frequency during locomotion. Neuron. 2001; 31:617–630. [PubMed: 11545720]
49. Ward A, Liu J, Feng Z, Xu XZ. Light-sensitive neurons and channels mediate phototaxis in C. elegans. Nat Neurosci. 2008; 11:916–922. [PubMed: 18604203]
50. Richmond JE, Jorgensen EM. One GABA and two acetylcholine receptors function at the C. elegans neuromuscular junction. Nat Neurosci. 1999; 2:791–797. [PubMed: 10461217]

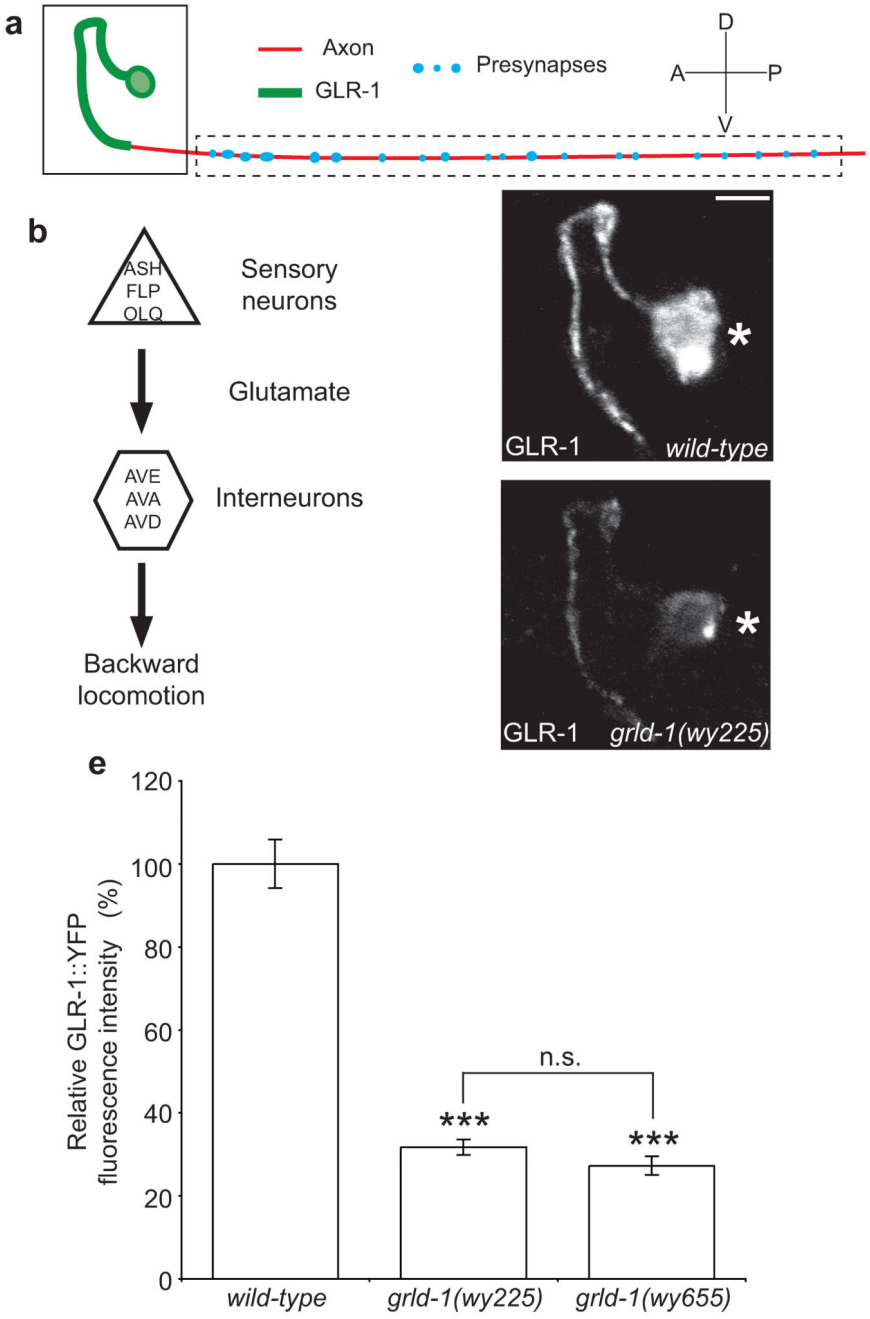

Figure 1. *grld-1(wy225)* mutants have decreased levels of GLR-1 in AVE

(**a**) Schematic diagram of AVE: green represents postsynaptic segment; red denotes axonal segment of the AVE process. (**b**) Circuit diagram of the nose-touch avoidance response. The sensory neurons ASH, FLP, and OLQ release glutamate to their *glr-1*-expressing synaptic partners, the interneurons AVE, AVA, and AVD. AVE, AVA, and AVD synapse onto the A-type motor neurons that stimulate the body wall muscles resulting in backwards locomotion. (**c, d**) Representative confocal image of GLR-1::YFP fluorescence in AVE of L2-stage wild-type (**c**) and *grld-1(wy225)* animals (**d**). The same region as boxed in a is

shown. Asterisk, AVE cell body. Scale bar, 2 μm. (**e**) Comparison of GLR-1::YFP fluorescence intensity (normalized to wild-type) between wild-type, *grld-1(wy225)*, and *grld-1(wy655)* worms. $n > 20$. Error bars, s.e.m. ***P < 0.001, n.s. = not significant, compared to wild-type animals unless otherwise depicted, *t*-test.

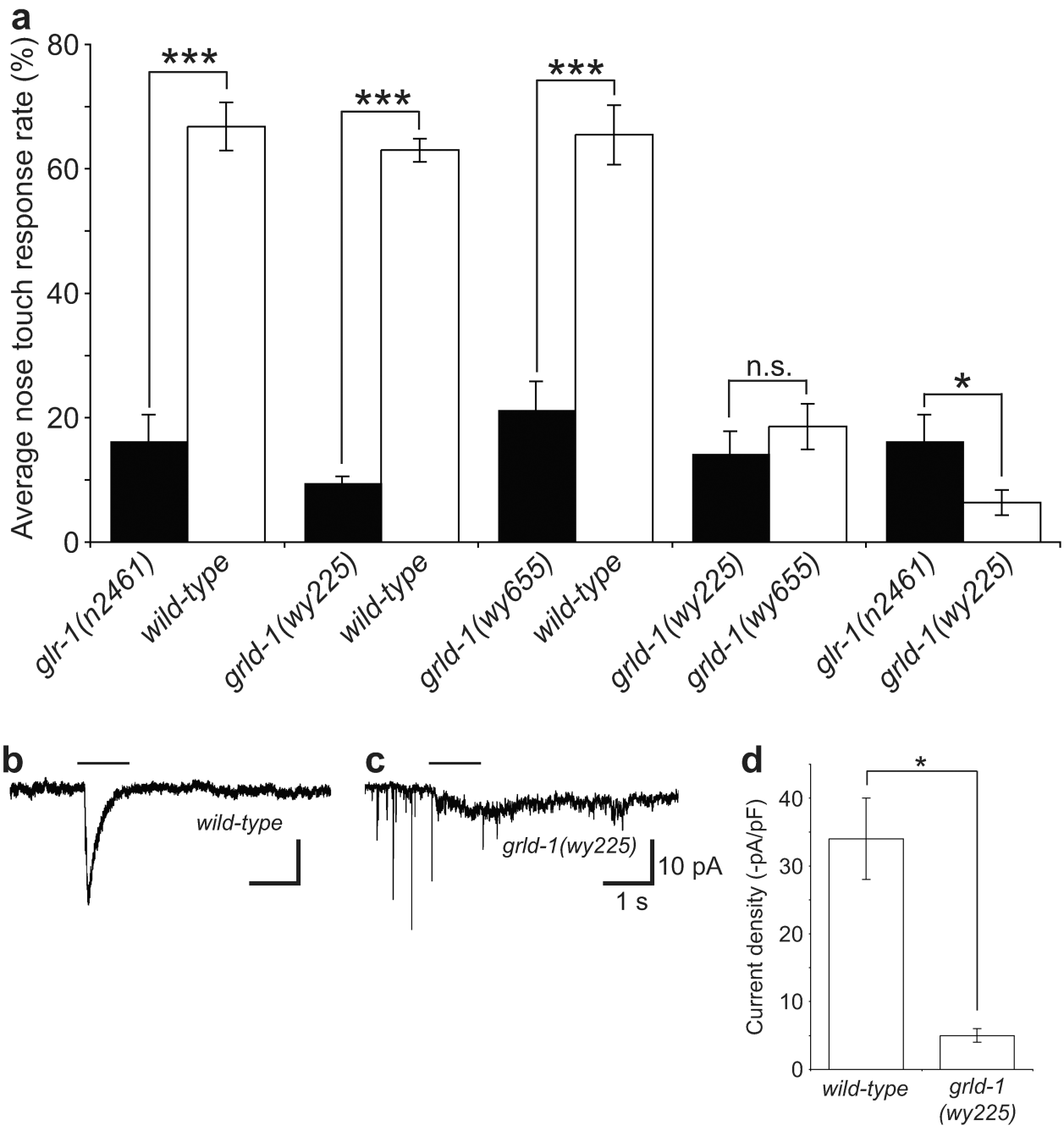

Figure 2. *grld-1* mutants are nose-touch defective and exhibit decreased glutamate-gated currents

(**a**) Comparison of nose-touch behavioural response between wild-type, *glr-1(n2461)*, *grld-1(wy225)*, and *grld-1(wy655)* animals. The compared genotypes were assayed on the same days. Wild-type compared to *grld-1(wy225)* mutants: $n = 177$, other comparisons: $n > 20$. Error bars, s.e.m. ***P < 0.001, *P < 0.05, *t*-test. (**b, c**) *In vivo* whole-cell patch-clamp of AVE to measure inward currents with application of 1 mM glutamate (black line). Sample inward currents of wild-type (**b**) and *grld-1(wy225)* (**c**) AVE. The downward

"spikes" in some traces are typical for many worm neurons that show very high input resistance (~4 GOhm is typical)[43]. (**d**) Comparison of current intensity between wild-type (n = 22) and *grld-1(wy225)* (n = 8) animals. Error bars, s.e.m. *P < 0.05, ANOVA.

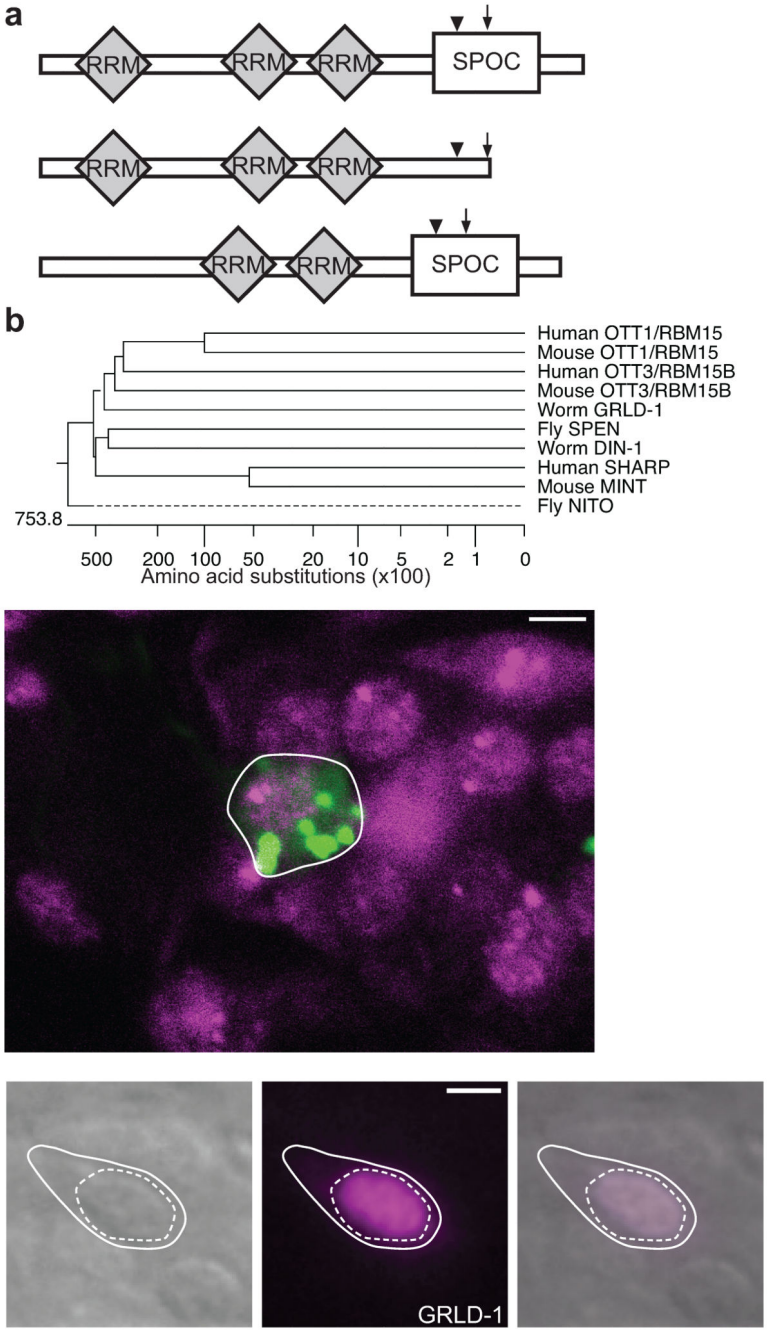

Figure 3. GRLD-1 is a member of the SPEN family

(**a**) Schematic domain structure of the three isoforms of GRLD-1. The arrow indicates the position of the molecular lesion of *grld-1(wy225)* and the arrowhead indicates that of *grld-1(wy655)*. (**b**) Phylogenetic analysis of GRLD-1 and SPEN family members. (**c**) *grld-1* is expressed in AVE. mCherry (pseudo-colored green) is expressed in AVE by the *opt-3* promoter (outlined by white line) and GFP-tagged GRLD-1 (pseudo-colored magenta) is expressed with fosmid recombineering. The nerve ring is anterior to AVE. The image is a single confocal plane (~1 μm) of an L2-staged worm. Scale bar, 2 μm. (**d–f**) GFP::GRLD-1

localizes to the nucleus when expressed in AVE. Solid line, cell body; dashed line, nucleus. DIC image of AVE (**d**), pseudo-colored GFP-tagged GRLD-1 (**e**), and overlay (**f**) at the L4 stage. Scale bar, 2 μm.

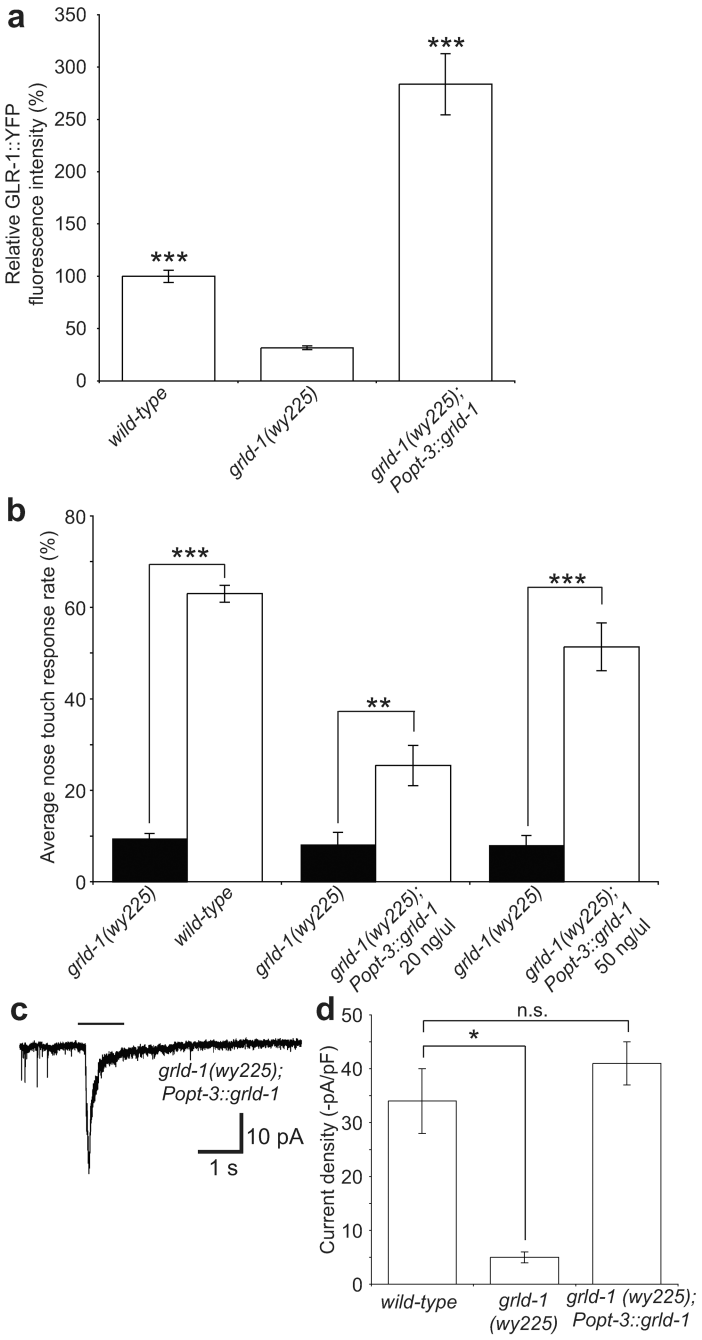

Figure 4. GRLD-1 acts cell autonomously in AVE

(**a**) Comparison of GLR-1::YFP fluorescence intensity (normalized to wild-type) between wild-type, *grld-1* mutants, and *grld-1* mutants expressing *grld-1* cDNA under the *opt-3* promoter. $n > 20$. Error bars, s.e.m. ***P < 0.001, compared to *grld-1* mutants, *t*-test. (**b**) Analysis of nose-touch behavior with expression of *grld-1* cDNA under the *opt-3* promoter. Wild-type compared to *grld-1* mutants: $n = 177$, transgenic animals compared to *grld-1* mutants: $n > 20$. The compared genotypes were assayed on the same days. Error bars, s.e.m. ***P < 0.001, **P < 0.01, *t*-test. (**c, d**) *In vivo* whole-cell patch-clamp of AVE in *grld-1*

mutants expressing *grld-1* cDNA under the *opt-3* promoter. Sample inward current of *grld-1(wy225)* expressing *grld-1* cDNA under the *opt-3* promoter (**c**), black line represents application of 1 mM glutamate. (**d**) Comparison of current intensity between wild-type (n = 22), *grld-1(wy225)* (n = 8), and *grld-1(wy225)* mutants expressing *grld-1* cDNA under the *opt-3* promoter (n = 15) animals. Error bars, s.e.m. *P < 0.05, n.s. = not significant, ANOVA test.

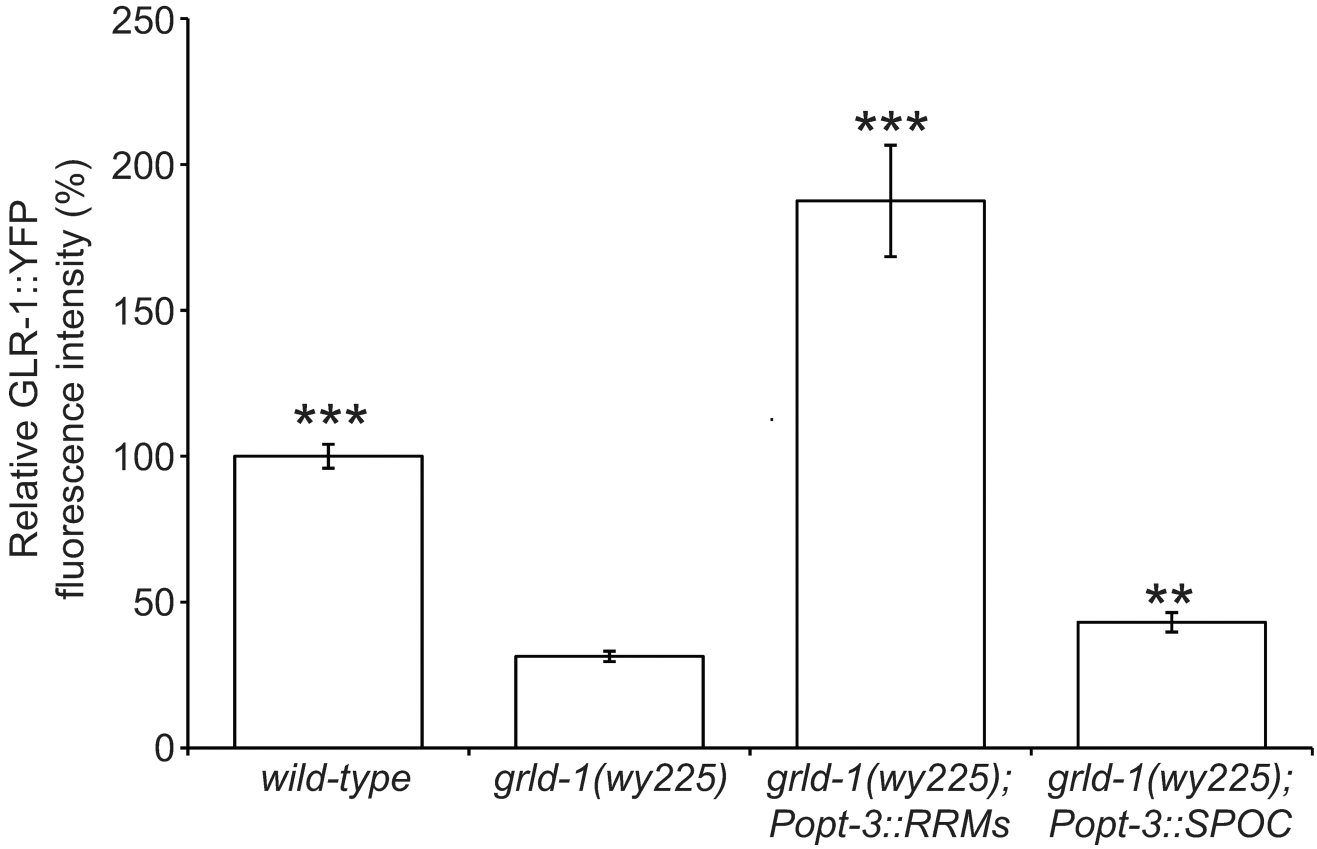

Figure 5. The GRLD-1 RRMs are sufficient to rescue GLR-1 levels in AVE

Comparison of GLR-1::YFP fluorescence intensity (normalized to wild-type) between wild-type, *grld-1* mutants, *grld-1* mutants expressing *grld-1 RRMs* cDNA under the *opt-3* promoter, and *grld-1* mutants expressing *grld-1 SPOC* cDNA under the *opt-3* promoter.

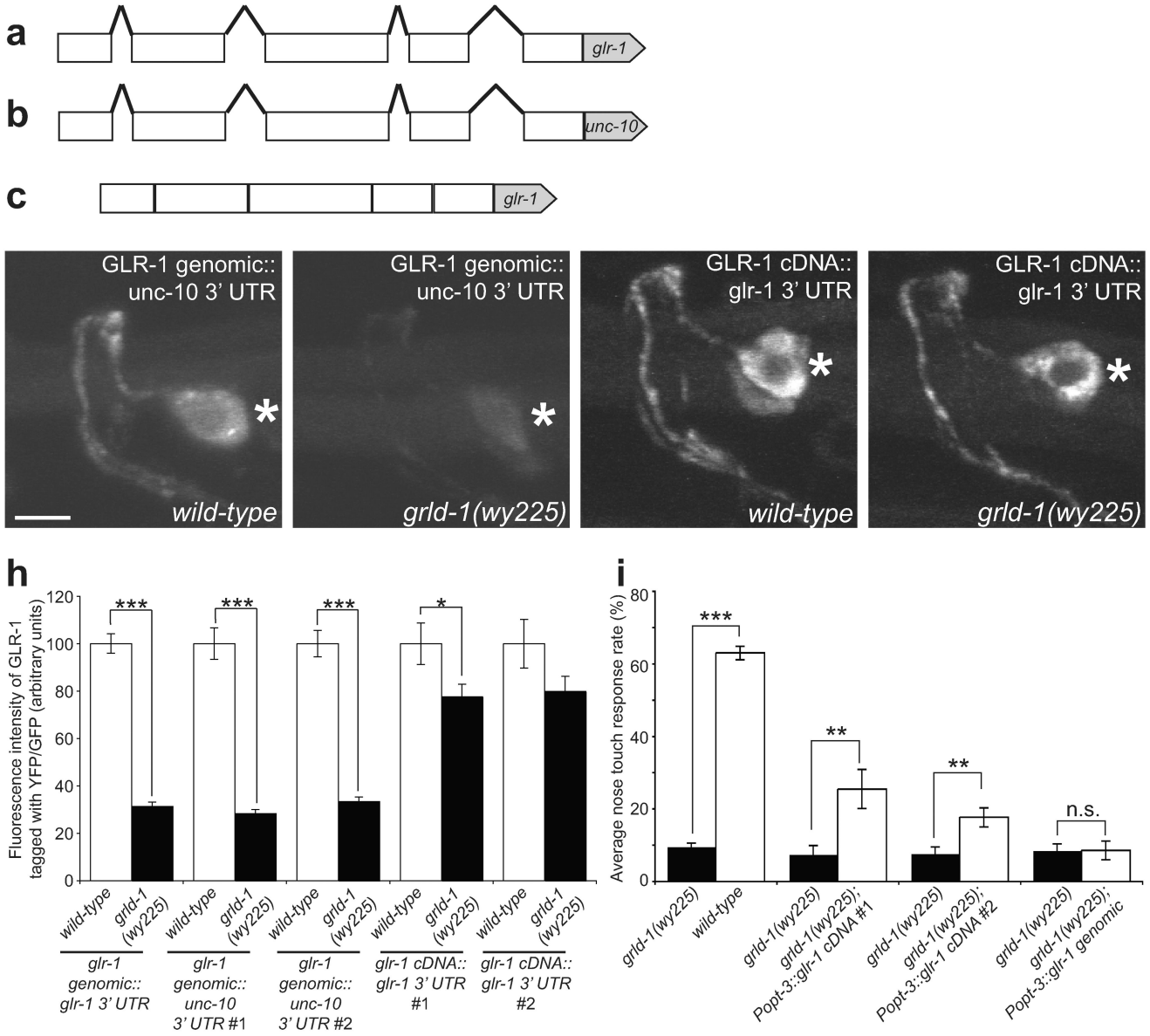

Figure 6. Expression of *glr-1* cDNA bypasses the requirement for *grld-1*

(**a–c**) Schematic cartoon of the rescuing constructs. Lines, introns; boxes, exons; pentagons, 3' UTR. Note this *glr-1* depiction does not contain all of the introns and exons. *glr-1 genomic::glr-1 3' UTR*: all endogenous exons, introns, and 3' UTR (**a**). *glr-1 cDNA::unc-10 3' UTR*: all endogenous exons and introns, *unc-10 3' UTR* (**b**). *glr-1 cDNA::glr-1 3' UTR*: all endogenous exons, no introns, *glr-1 3' UTR* (**c**). (**d–g**) Representative L2-stage wild-type animals (**d, f**) and *grld-1(wy225)* mutants (**e, g**). Asterisk, AVE cell body. Scale bar, 2 μm. (**h**) Effectiveness of the *glr-1* constructs in rescuing the GLR-1 fluorescent phenotypes. The *glrd-1(wy225)* intensities were normalized to their respective expression constructs. $n \geq 19$. Error bars, s.e.m. ***P < 0.001, *P < 0.05, *t*-test. (**i**) Effectiveness of the *glr-1* constructs in rescuing the nose-touch behavior defect. The compared genotypes were assayed on the same days. $n \geq 20$. Error bars, s.e.m.***P < 0.001, **P < 0.01, *t*-test.

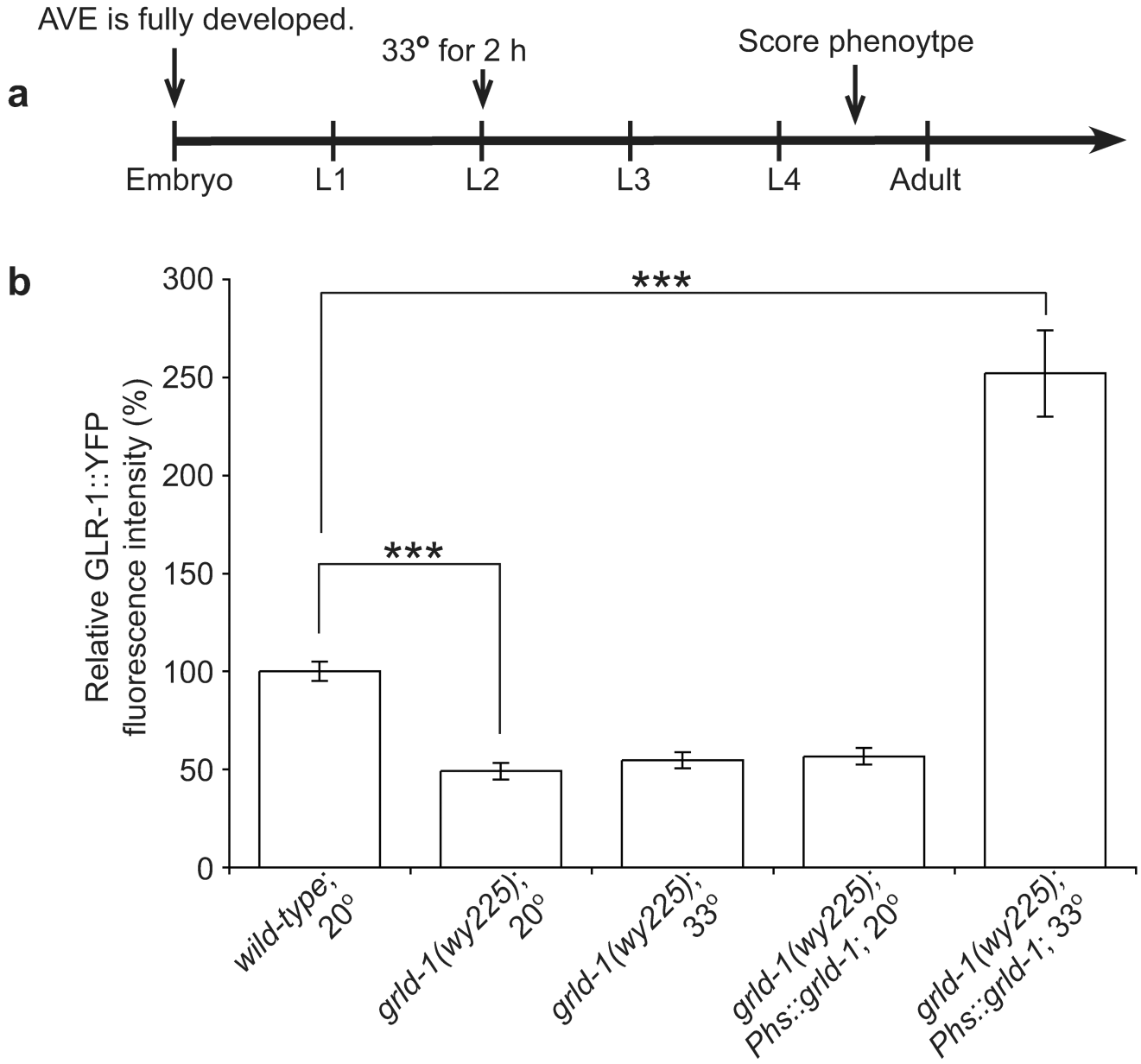

Figure 7. Expression of *grld-1* after initial development can rescue GLR-1 levels

(**a**) Schematic of heat-shock experimental timeline. Animals were heat-shocked for 2 hours at 33° during the L2 stage or were not heat-shocked (kept at 20°). GLR-1::YFP fluorescent intensity was measured 18 hours after the heat-shock. (**b**) Comparison of GLR-1::YFP fluorescence intensity (normalized to wild-type) of wild type without heat-shock, *grld-1* mutants without heat-shock, *grld-1* mutants with heat-shock, *grld-1* mutants expressing *grld-1* cDNA under the *hsp16-2* and *hsp16-41* promoters (*Phs*) without heat-shock, and *grld-1* mutants expressing *grld-1* cDNA under the *hsp16-2* and *hsp16-41* promoters with heat-shock. $n = 20$. Error bars, s.e.m. ***P < 0.001, *t*-test.